High activation of STAT5A drives peripheral T-cell lymphoma and leukemia

Barbara Maurer,[1,2,3] Harini Nivarthi,[4] Bettina Wingelhofer,[1,2] Ha Thi Thanh Pham,[1,2] Michaela Schlederer,[1,5] Tobias Suske,[2] Reinhard Grausenburger,[3] Ana-Iris Schiefer,[5] Michaela Prchal-Murphy,[3] Doris Chen,[4] Susanne Winkler,[1] Olaf Merkel,[5] Christoph Kornauth,[5] Maximilian Hofbauer,[1] Birgit Hochgatterer,[1] Gregor Hoermann,[6] Andrea Hoelbl-Kovacic,[3] Jana Prochazkova,[4] Cosimo Lobello,[7] Abbarna A. Cumaraswamy,[8] Johanna Latzka,[9] Melitta Kitzwögerer,[10] Andreas Chott,[11] Andrea Janikova,[12] Šárka Pospíšilova,[7,12] Joanna I. Loizou,[4] Stefan Kubicek,[4] Peter Valent,[13] Thomas Kolbe,[14,15] Florian Grebien,[1,16] Lukas Kenner,[1,5,17] Patrick T. Gunning,[7] Robert Kralovics,[4] Marco Herling,[18] Mathias Müller,[2] Thomas Rülicke,[19] Veronika Sexl[3] and Richard Moriggl[1,2,20]

[1]Ludwig Boltzmann Institute for Cancer Research, Vienna, Austria; [2]Institute of Animal Breeding and Genetics, University of Veterinary Medicine Vienna, Vienna, Austria; [3]Institute of Pharmacology and Toxicology, University of Veterinary Medicine Vienna, Vienna, Austria; [4]CeMM Research Center for Molecular Medicine of the Austrian Academy of Sciences, Vienna, Austria; [5]Department of Clinical Pathology, Medical University of Vienna, Vienna, Austria; [6]Department of Laboratory Medicine, Medical University of Vienna, Vienna, Austria; [7]Central European Institute of Technology (CEITEC), Center of Molecular Medicine, Masaryk University, Brno, Czech Republic; [8]Department of Chemistry, University of Toronto Mississauga, Mississauga, Ontario, Canada; [9]Karl Landsteiner Institute of Dermatological Research, St. Poelten, Austria and Department of Dermatology and Venereology, Karl Landsteiner University for Health Sciences, St. Poelten, Austria; [10]Department of Clinical Pathology, Karl Landsteiner University of Health Sciences, St. Poelten, Austria; [11]Institute of Pathology and Microbiology, Wilhelminenspital, Vienna, Austria; [12]Department of Internal Medicine – Hematology and Oncology, Faculty of Medicine Masaryk University and University Hospital Brno, Brno, Czech Republic; [13]Department of Internal Medicine I, Division of Hematology and Hemostaseology and Ludwig Boltzmann Cluster Oncology, Medical University of Vienna, Vienna, Austria; [14]Biomodels Austria, University of Veterinary Medicine Vienna, Vienna, Austria; [15]IFA-Tulln, University of Natural Resources and Applied Life Sciences, Tulln, Austria; [16]Institute of Medical Biochemistry, University of Veterinary Medicine Vienna, Vienna, Austria; [17]Unit of Laboratory Animal Pathology, University of Veterinary Medicine Vienna, Vienna, Austria; [18]Department I of Internal Medicine, Center for Integrated Oncology (CIO) Köln-Bonn, Excellence Cluster for Cellular Stress Response and Aging-Associated Diseases (CECAD), Center for Molecular Medicine Cologne (CMMC), University of Cologne, Cologne, Germany; [19]Institute of Laboratory Animal Science, University of Veterinary Medicine Vienna, Vienna, Austria and [20]Medical University of Vienna, Vienna, Austria

 doi:10.3324/haematol.2019.216986

Received: January 18, 2019.

Accepted: May 21, 2019.

Pre-published: May 23, 2019.

Correspondence: *RICHARD MORIGGL* - richard.moriggl@vetmeduni.ac.at

Supplementary Information

High activation of STAT5A drives peripheral T-cell lymphoma and leukemia

Barbara Maurer[1,2,3], Harini Nivarthi[4], Bettina Wingelhofer[1,2], Ha Thi Thanh Pham[1,2], Michaela Schlederer[1,5], Tobias Suske[2], Reinhard Grausenburger[3], Ana-Iris Schiefer[5], Michaela Prchal-Murphy[3], Doris Chen[4], Susanne Winkler[1], Olaf Merkel[5], Christoph Kornauth[5], Maximilian Hofbauer[1], Birgit Hochgatterer[1], Gregor Hoermann[6], Andrea Hoelbl-Kovacic[3], Jana Prochazkova[4], Cosimo Lobello[7], Abbarna A. Cumaraswamy[8], Johanna Latzka[9], Melitta Kitzwögerer[10], Andreas Chott[11], Andrea Janikova[12], Šárka Pospíšilova[7,12], Joanna I. Loizou[4], Stefan Kubicek[4], Peter Valent[13], Thomas Kolbe[14,15], Florian Grebien[1,16], Lukas Kenner[1,5,17], Patrick T. Gunning[7], Robert Kralovics[4], Marco Herling[18], Mathias Müller[2], Thomas Rülicke[19], Veronika Sexl[3], and Richard Moriggl[1,2,20]

Supplementary Figures and Figure Legends

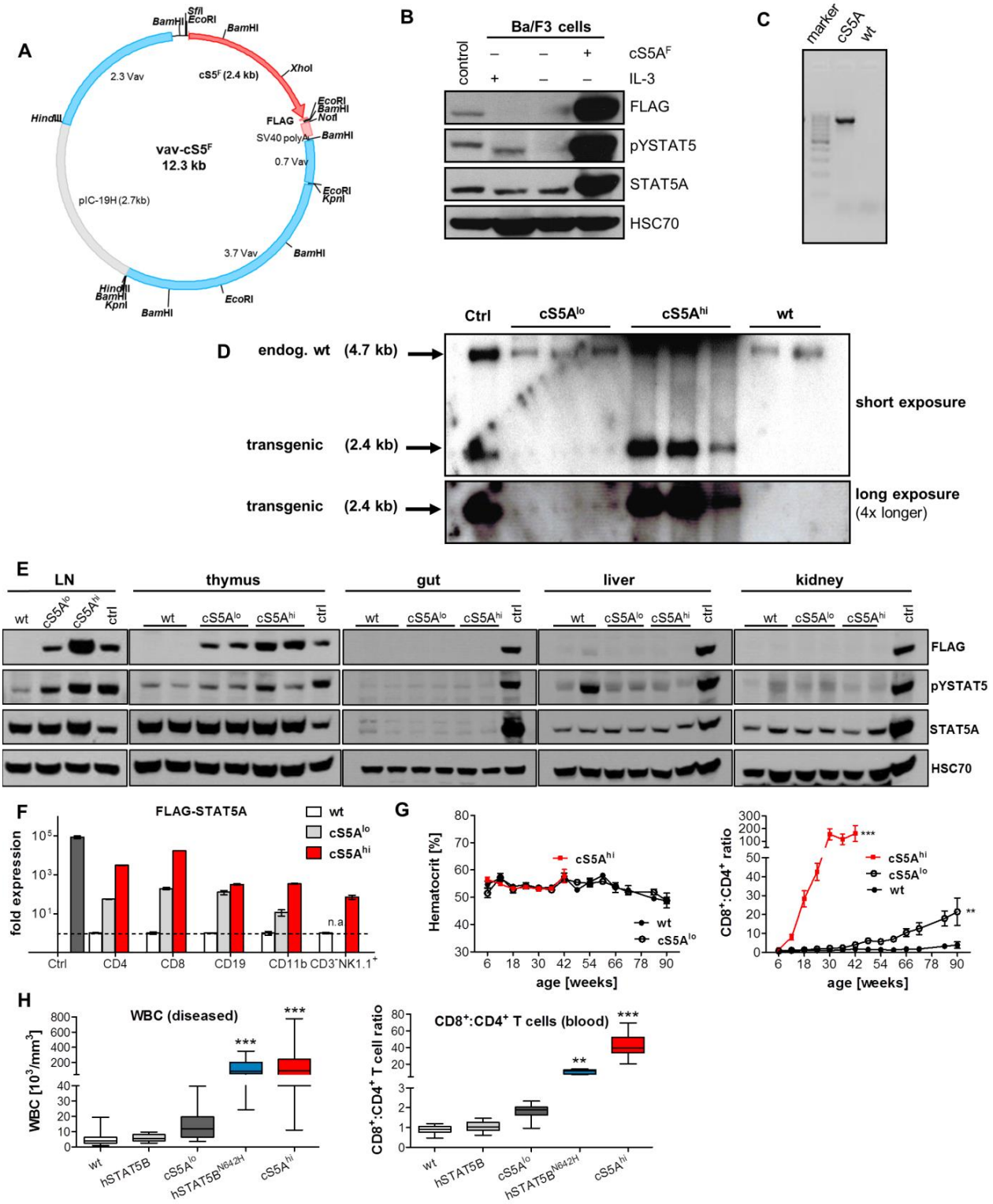

Supplementary Figure 1. Generation of transgenic mice expressing cS5^F under the *vav*-promoter

A. Schematic representation of the cS5A^F (vav-cS5^F) construct with restriction sites. B. Western blot on whole cell extracts isolated from Ba/F3 cells starved overnight with or without IL-3 stimulation (5 ng/ml) and Ba/F3 cS5A^F cells grown without IL-3 analyzed for FLAG, pYSTAT5 and STAT5A expression. HSC70 served as loading control. Control: Protein from 3T3 cells expressing cS5^F-FLAG. C. cS5A^F positive offspring was detected by a 952 bp PCR amplification fragment on genomic DNA

using transgene specific primers. D. Detection of *cS5A*^{F} copy number in transgenic mice (n=3) by Southern blot signal intensity. 4.7 kB band refers to endogenous *Stat5* and a 2.4 kB band refers to the *cS5*^{F} transgene. DNA from wt littermates (n=2) and from mice expressing *cS5*^{F} under endogenous promoter were used as controls. E. Western blot on cell lysates of lymph nodes, thymi, gut, liver and kidney from 6-week-old wt, cS5A^{lo} and cS5A^{hi} mice (n=2/genotype) using antibodies to FLAG, phosphotyrosine (Y694)-STAT5 (pYSTAT5) and STAT5A. HSC70 was used as loading control and cS5^{F}-FLAG expressing Ba/F3 cells served as positive control. Representative blots of 4 experiments. F. qPCR analysis showing fold change in mRNA expression of FLAG-tagged *STAT5A* isolated from FACS sorted CD8^{+}, CD4^{+}, CD19^{+} (spleen), and CD11b^{+} cells (bone marrow) from 8-week-old cS5A^{lo}, cS5A^{hi} and wt mice (n=3/genotype) as well as cultured and FACS-sorted natural killer (NK) cells from 7-week-old wt (n=4) and cS5A^{hi} mice (n=3), mRNA isolated from diseased cS5A^{hi} spleen was used as positive control. Gene expression was calculated relative to the housekeeping gene *Gapdh* and normalized to the expression of wt. Broken line at 1-fold indicates zero FLAG-tagged *STAT5A* mRNA expression as in wt cells. G. Left: Hematocrit in peripheral blood obtained in six-week-intervals from wt (n≥6), cS5A^{lo} (n≥8) and cS5A^{hi} (n≥10) mice for 66 weeks (cS5A^{hi} until 42 weeks). Right: flow cytometric analysis of the same peripheral blood samples showing %CD8:%CD4 T-cell ratio (unpaired t-test wt vs cS5A^{lo} P=0.0068, wt vs cS5A^{hi} P=0.0008). H. White blood cell (WBC) count and CD8^{+}:CD4^{+} T-cell ratio in peripheral blood of diseased cS5A^{hi} (n≥10) and hSTAT5B^{N642H} (n≥5) mice and age-matched controls (wt [n≥22], cS5A^{lo} [n≥8], hSTAT5B [n≥12], one-way ANOVA with Tukey's multiple comparison test compared to wt).

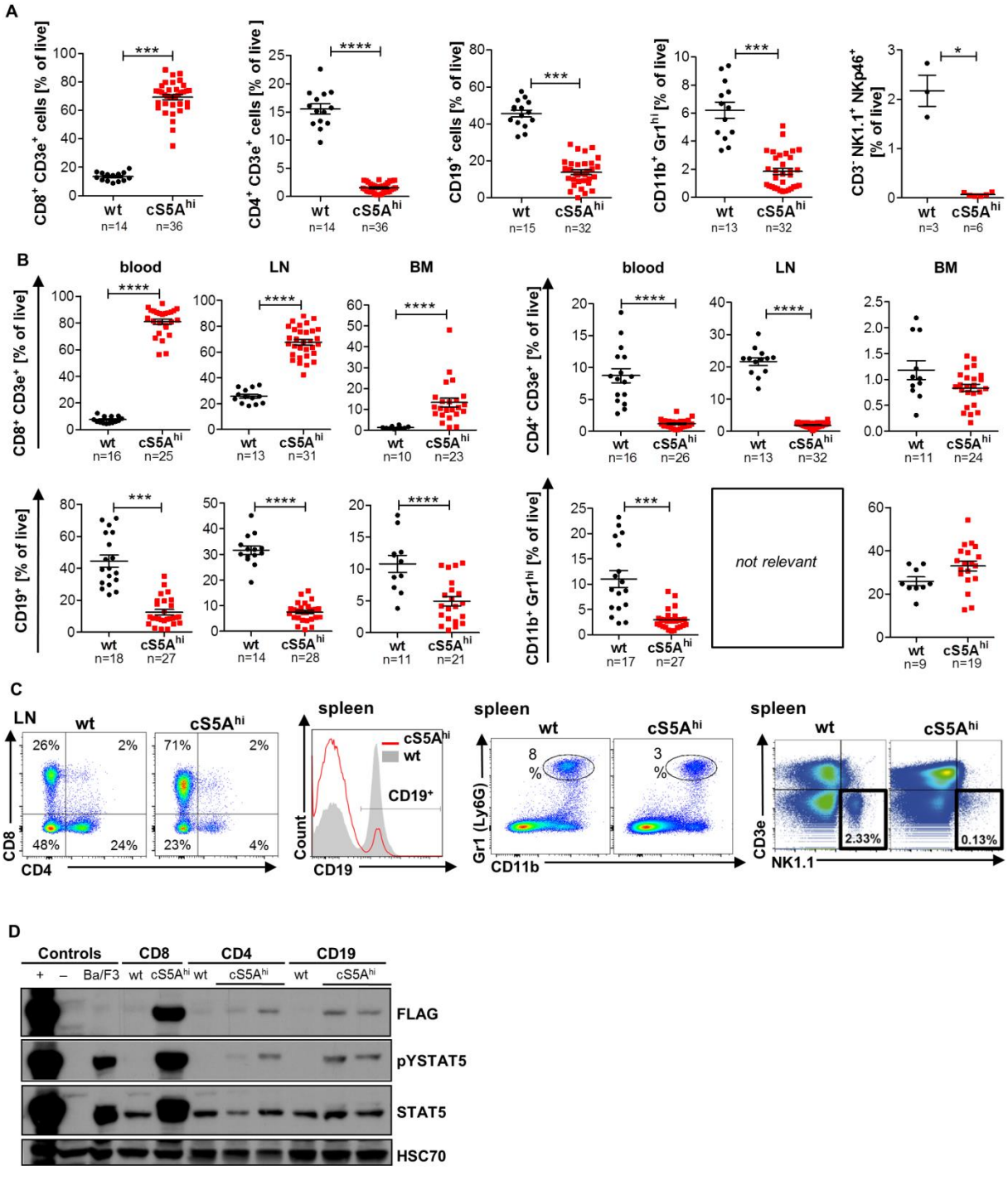
A
CD8+ CD3e+ cells [% of live]
CD4+ CD3e+ cells [% of live]
CD19+ cells [% of live]
CD11b+ Gr1hi [% of live]
CD3- NK1.1+ NKp46+ [% of live]
wt
cS5Ahi
n=14
n=36
n=15
n=32
n=13
n=3
n=6
B
blood
LN
BM
CD8+ CD3e+ [% of live]
CD4+ CD3e+ [% of live]
CD19+ [% of live]
CD11b+ Gr1hi [% of live]
n=16
n=25
n=13
n=31
n=10
n=23
n=26
n=11
n=24
n=18
n=27
n=14
n=28
n=21
n=17
n=27
n=9
n=19
not relevant
C
LN
spleen
CD8
CD4
CD19
Count
CD19+
Gr1 (Ly6G)
CD11b
CD3e
NK1.1
26%
2%
71%
48%
24%
23%
4%
8 %
3 %
2.33%
0.13%
D
Controls
CD8
CD4
CD19
Ba/F3
FLAG
pYSTAT5
STAT5
HSC70

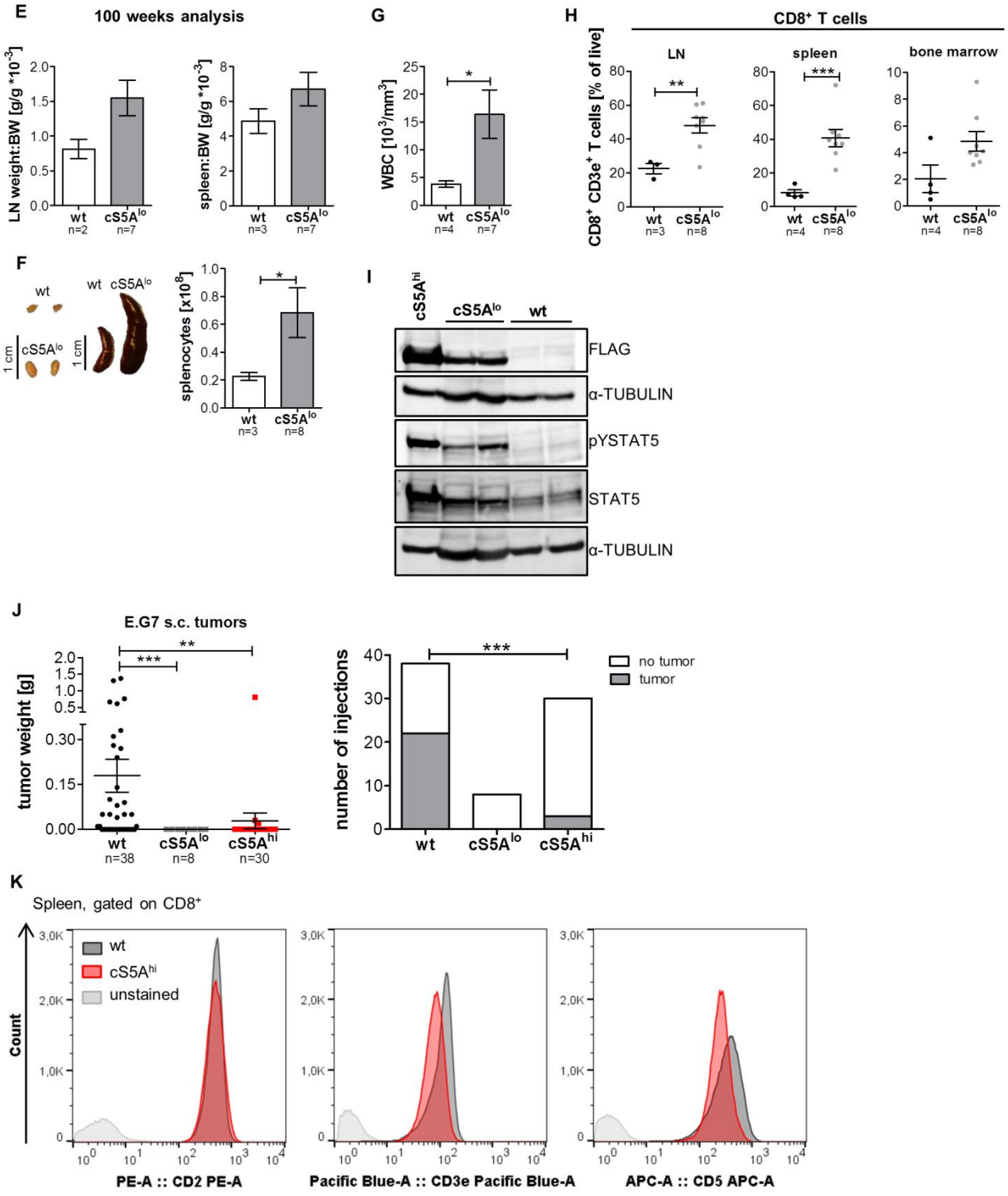
E
100 weeks analysis
LN weight:BW [g/g *10-3]
spleen:BW [g/g *10-3]
wt n=2
cS5Alo n=7
wt n=3
cS5Alo n=7
G
WBC [10^3/mm^3]
wt n=4
cS5Alo n=7
H
CD8+ T cells
CD8+ CD3e+ T cells [% of live]
LN
spleen
bone marrow
wt n=3
cS5Alo n=8
wt n=4
cS5Alo n=8
wt n=4
cS5Alo n=8
F
wt
cS5Alo
1 cm
splenocytes [x10^8]
wt n=3
cS5Alo n=8
I
cS5Ahi
cS5Alo
wt
FLAG
α-TUBULIN
pYSTAT5
STAT5
α-TUBULIN
J
E.G7 s.c. tumors
tumor weight [g]
wt n=38
cS5Alo n=8
cS5Ahi n=30
number of injections
no tumor
tumor
wt
cS5Alo
cS5Ahi
K
Spleen, gated on CD8+
wt
cS5Ahi
unstained
Count
PE-A :: CD2 PE-A
Pacific Blue-A :: CD3e Pacific Blue-A
APC-A :: CD5 APC-A

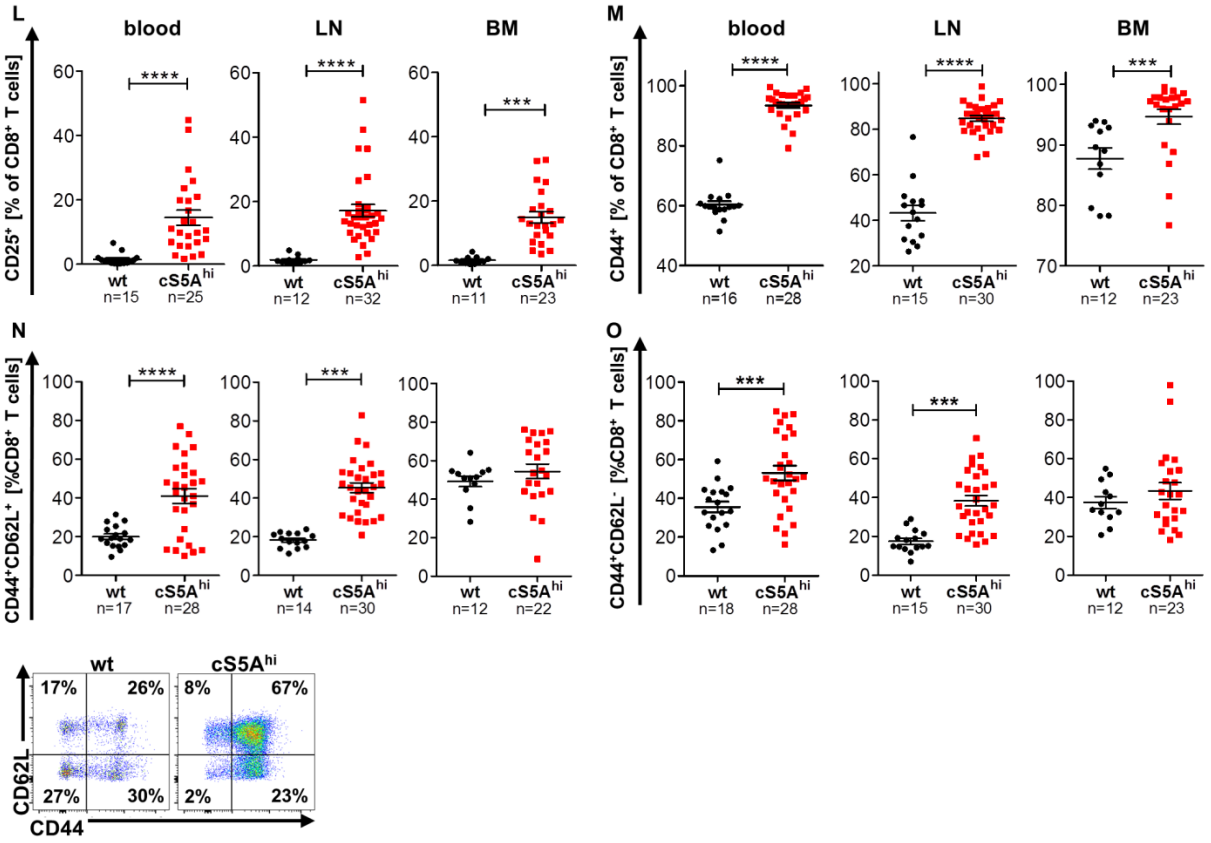

P

cS5A^hi vs cS5A^lo

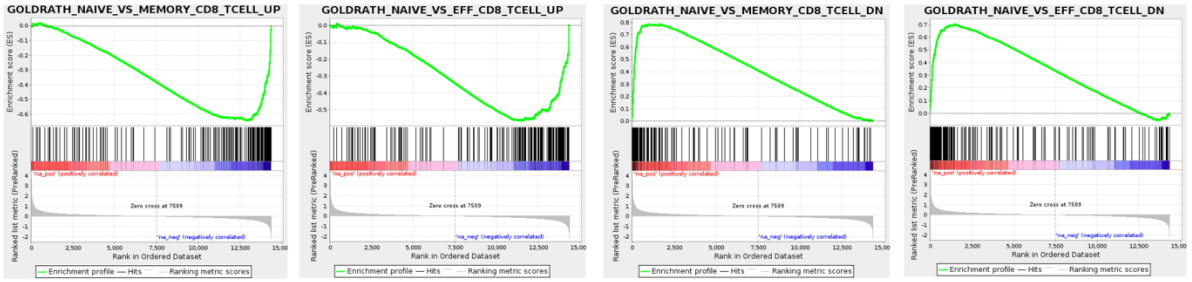

NES…-2.435
FDR…0

NES…-2.184
FDR…0

NES…2.813
FDR…0

NES…2.534
FDR…0

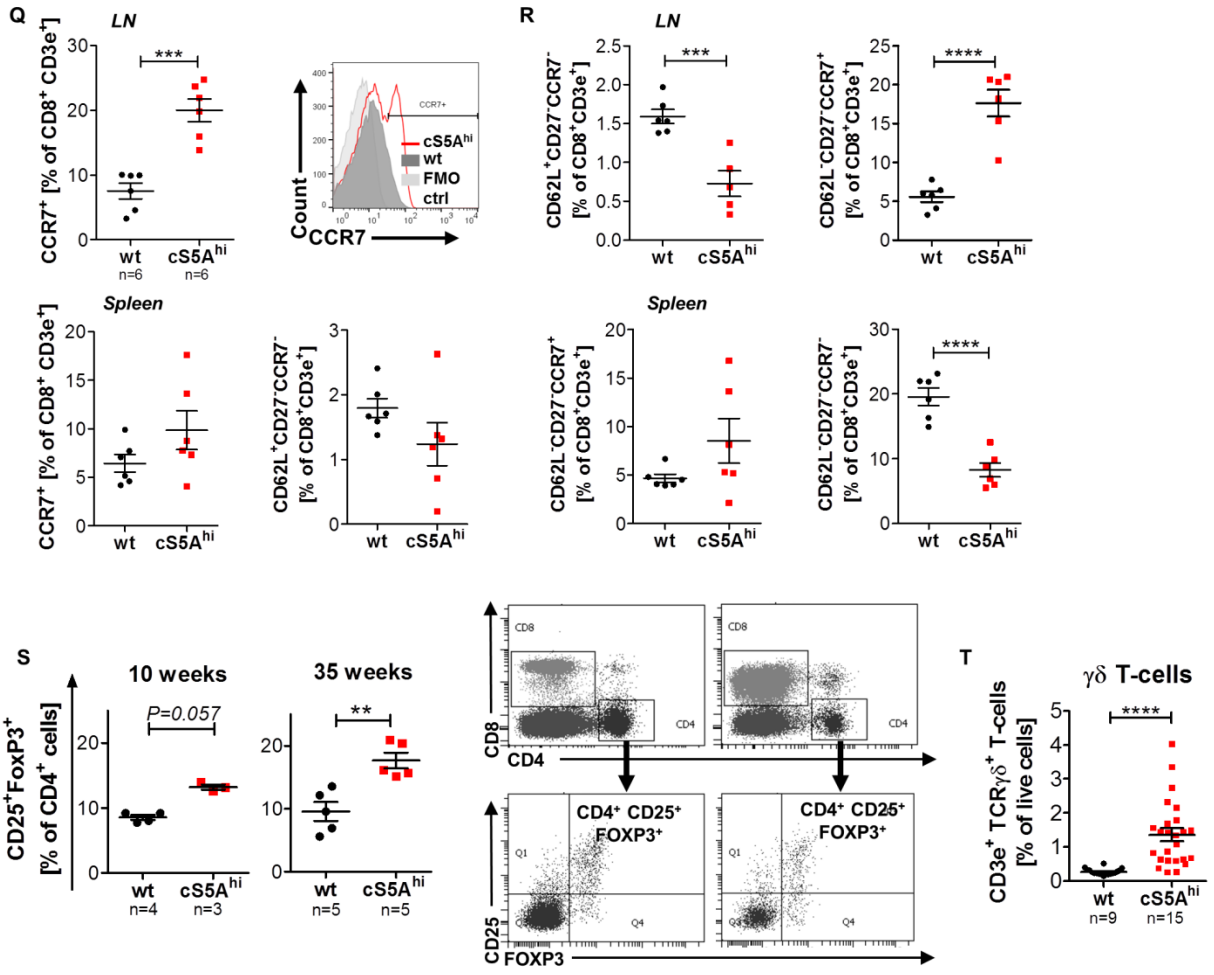

Supplementary Figure 2: High STAT5A activation leads to a neoplastic expansion of mature CD8$^+$ T cells

A. Flow cytometric analysis on relative CD8$^+$ T-cells (P=0.0001), CD4$^+$ T-cells (P<0.0001, both unpaired t-test with Welch's correction), B-cells (P=0.0001), CD11b$^+$Gr1^{hi} (P=0.0001, unpaired t-test) and NK-cells (P=0.0218, both unpaired t-test with Welch's correction). B. Relative fraction of (top) CD8$^+$ and CD4$^+$ T-cells, (bottom) CD19$^+$ B-cells and CD11b$^+$Gr1^{hi} granulocytes in peripheral blood, lymph nodes, and bone marrow of diseased cS5A^{hi} mice and wt littermates determined by flow cytometry. All unpaired t-test with Welch's correction besides CD19$^+$ bone marrow and CD11b$^+$Gr1^{hi} bone marrow unpaired t-test, all P<0.0001, except blood CD11b$^+$Gr1^{hi} cells P=0.0002, bone marrow CD4$^+$ T-cells and CD11b$^+$Gr1^{hi} cells not significant (n.s.), bone marrow B cells P=0.0003). CD11b$^+$Gr1^{hi} cells in lymph nodes were not significantly detectable. C. (Left) Representative dot plots of CD8$^+$ and CD4$^+$ T-cells with gating (shown lymph nodes), (middle) histogram of CD19 expression in wt and cS5A^{hi} splenocytes and (right) dot plots of CD11b$^+$Gr1^{hi} cells and NK-cells with gating (shown spleen, right panel). D. Immunoblot on whole cell lysates of CD8$^+$, CD4$^+$ and CD19$^+$ MACS sorted cells from 10-week-old wt (n=5) and cS5A^{hi} mice (n=4) for FLAG, pYSTAT5 and STAT5 expression. HSC70 served as loading control, cS5A^F transfected Ba/F3 cells served as positive and *Stat5*$^{-/-}$ mouse embryonic fibroblasts (MEFs) as negative control. Representative blot of four experiments. E. Analysis of 100 weeks old cS5A^{lo} and wt mice. lymph nodes weight/body weight and spleen/body weight ratio, F. macroscopic appearance of lymph nodes and spleen (scale bar for 1 cm),

and splenocyte numbers in 100 weeks old wt ($n \geq 2$) and cS5A^{lo} ($n \geq 7$) mice (lower panel, P=0.04). G. White blood cell (WBC) count in peripheral blood (P=0.0288). H. Statistical summary of flow cytometry staining for CD8$^+$ T-cells on secondary hematopoietic organs (lymph nodes P=0.0098; spleen P=0.0003) (for E-H: All unpaired t-tests, except splenocyte number, white blood cell and CD8$^+$ splenocytes unpaired t-test with Welch's correction and %CD8 in bone marrow Mann Whitney test P=0.1091). I. Western blot of spleen cell lysates from 70 weeks old cS5A^{lo} (n=2) and wt mice (n=2) showing FLAG, pYSTAT5 and STAT5 expression. cS5A^{hi} spleen lysates were used as positive control and α-TUBULIN served as loading control. Representative blot of four experiments J. Tumor weight (left) and tumor incidence per injection (right) 24 days after 1*10^5 *s.c.* (subcutaneous) E.G7 cell injection (wt and cS5A^{hi} 3 experiments, cS5A^{lo} one experiment, left: Kruskal-Wallis and Dunn's Multiple Comparison, right Logistic Regression). K. Histograms of CD2, CD3e and CD5 flow cytometry analysis of wt and cS5A^{hi} CD8$^+$ splenocytes (FlowJo v10). L. CD25$^+$, M. CD44$^+$, N. CD44$^+$CD62L$^+$ and O. CD44$^+$CD62L$^-$ CD8$^+$ T-cells expression in peripheral blood (left), lymph nodes (middle) and bone marrow (right) of diseased cS5A^{hi} mice and wt littermates determined by flow cytometry (L. and M. peripheral blood and lymph nodes P<0.0001, bone marrow CD8$^+$CD25$^+$ P<0.0001, CD8$^+$CD44$^+$ P=0.0009, N. peripheral blood P<0.0001, lymph nodes P<0.0001, bone marrow n.s., O. peripheral blood P=0.0005, lymph nodes P<0.0001, bone marrow n.s.). L-O all unpaired t-test with Welch's correction, L. peripheral blood and lymph nodes unpaired t-test, M. peripheral blood and bone marrow Mann-Whitney test. N (bottom) Representative CD62L/CD44 gating on CD8$^+$ splenocytes by FlowJo. P. Gene set enrichment analysis (GSEA) of genes up- or downregulated in cS5A^{hi} compared to cS5A^{lo} CD8$^+$ T-cells (n=5/genotype) on published naïve, memory and effector CD8$^+$ T-cell gene sets. Q. CCR7 expression on CD8$^+$ lymph nodes (top) or spleen (bottom) cells in diseased cS5A^{hi} and wt littermates determined by flow cytometry with representative histograms (P=0.0002, unpaired t-test). R. CD62L$^+$CD27$^-$CCR7$^-$ and CD62L$^-$CD27$^-$ CCR7$^+$ CD8$^+$ T-cells in lymph nodes (top, P=0.001 or P<0.0001) and spleen (bottom, P=0.13 or P<0.0001, unpaired t-test). S. Flow cytometric quantification of splenic T_{reg} cells in wt and cS5A^{hi} mice with gating strategy (35 weeks P=0.0032, unpaired t-test) and T: thymic γδ T cells (P<0.0001, unpaired t-test).

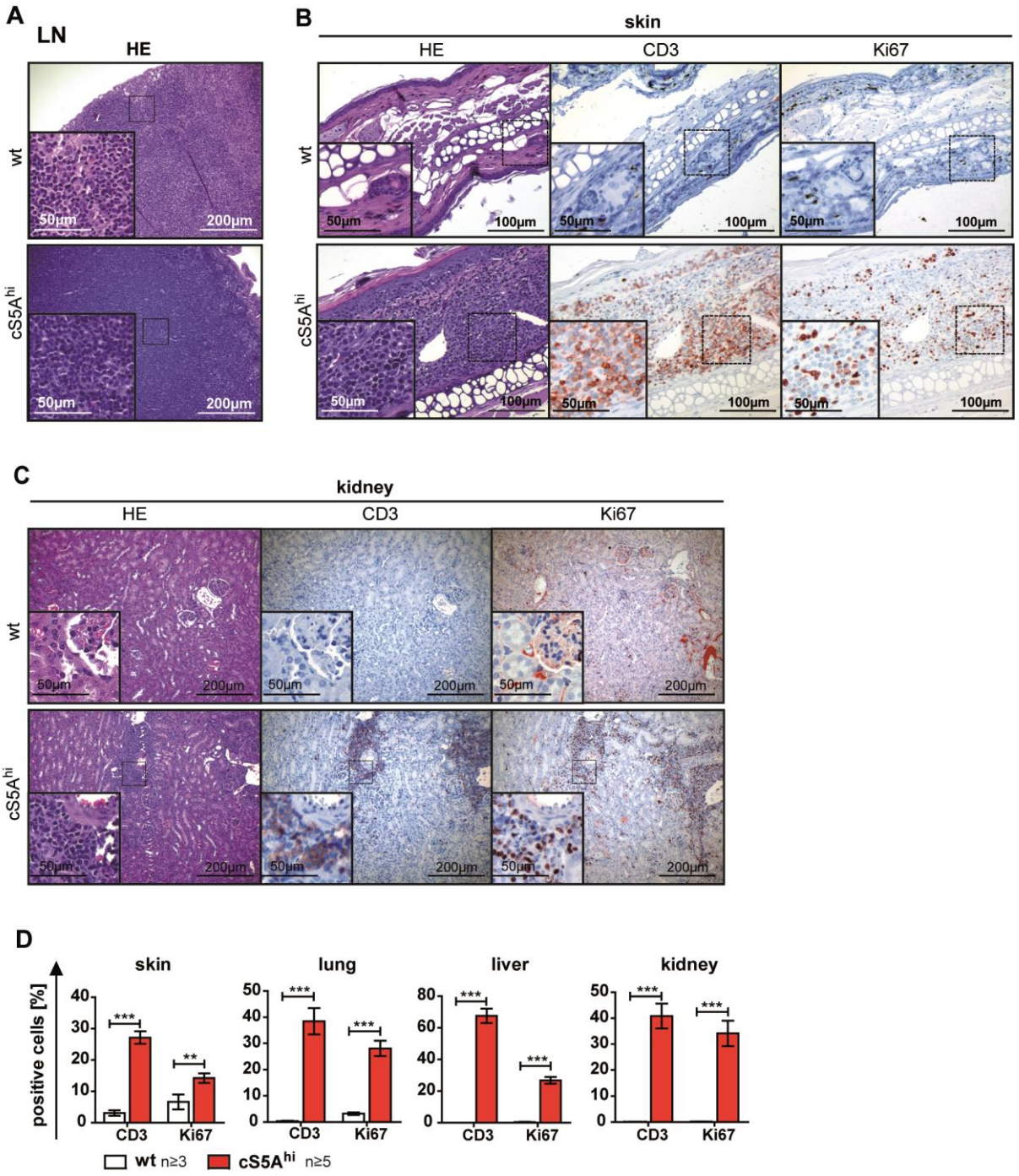

Supplementary Figure 3. Infiltrating T-cells disrupt lymph nodes and splenic architecture

A. Representative examples of wt lymph nodes and cS5A^{hi} lymphomas stained by HE (hematoxylin and eosin, corresponding CD3 staining in Figure 4A). HE (left), CD3 (middle) and Ki67 (right) staining on consecutive cuts of B. skin and D. kidney sections of age-matched wt and diseased cS5A^{hi} mice. Scale bars indicate 50, 100 or 200 µm. C. Diseased cS5A^{hi} mice with skin lesions. E. Quantification of infiltrating CD3^{+} and Ki67^{+} cells in skin, lung, liver and kidney in cS5A^{hi} and corresponding areas in wt mice (P<0.0001, except for skin %Ki67 positive cells P=0.0078, wt $n\geq3$, cS5A^{hi} $n\geq5$, all unpaired t-test).

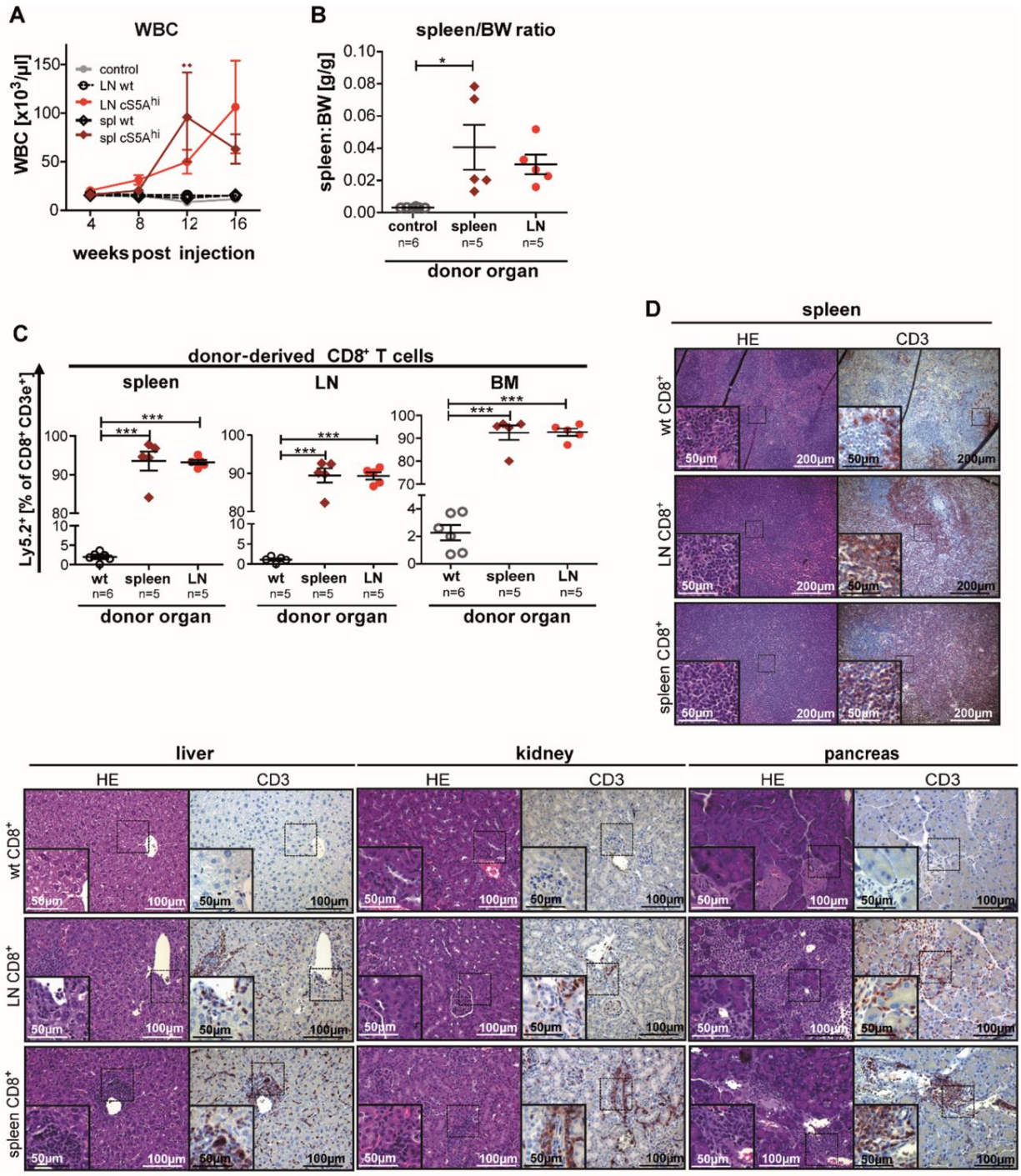

Supplementary Figure 4. Transplantable CD8$^+$ T-cell disease

A. White blood cell (WBC) count in recipient's blood measured post injection in 4-week-intervals for 16 weeks (n=6/organ source, control n=2, wt lymph nodes n=1, Two Way-ANOVA with Bonferroni Post Test). B. Endpoint analysis ($n\geq5$/group): Spleen/body weight ratio of wt CD8$^+$ T-cell recipients (control) and cS5A^{hi} spleen or lymph nodes CD8$^+$ T-cells recipients. C. Percentage of Ly5.2$^+$ cells gated on CD8$^+$CD3e$^+$ T-cells in spleen (left), lymph nodes (middle) and bone marrow (right) of control (wt lymph nodes and wt spleen recipients), spleen- and lymph nodes-derived cS5A^{hi} CD8 T-cell recipients. 1Way-ANOVA with Tukey's Multiple Comparison Test (B-C). D. Histological analysis (hematoxylin and eosin (HE) and anti-CD3 staining) on representative areas of spleen (top),

liver (left), kidney (middle) and pancreas (right) from wt or cS5A^{hi} CD8^{+} T-cell (isolated from lymph nodes or spleen) recipients. Scale bars indicate 50, 100 or 200 µm.

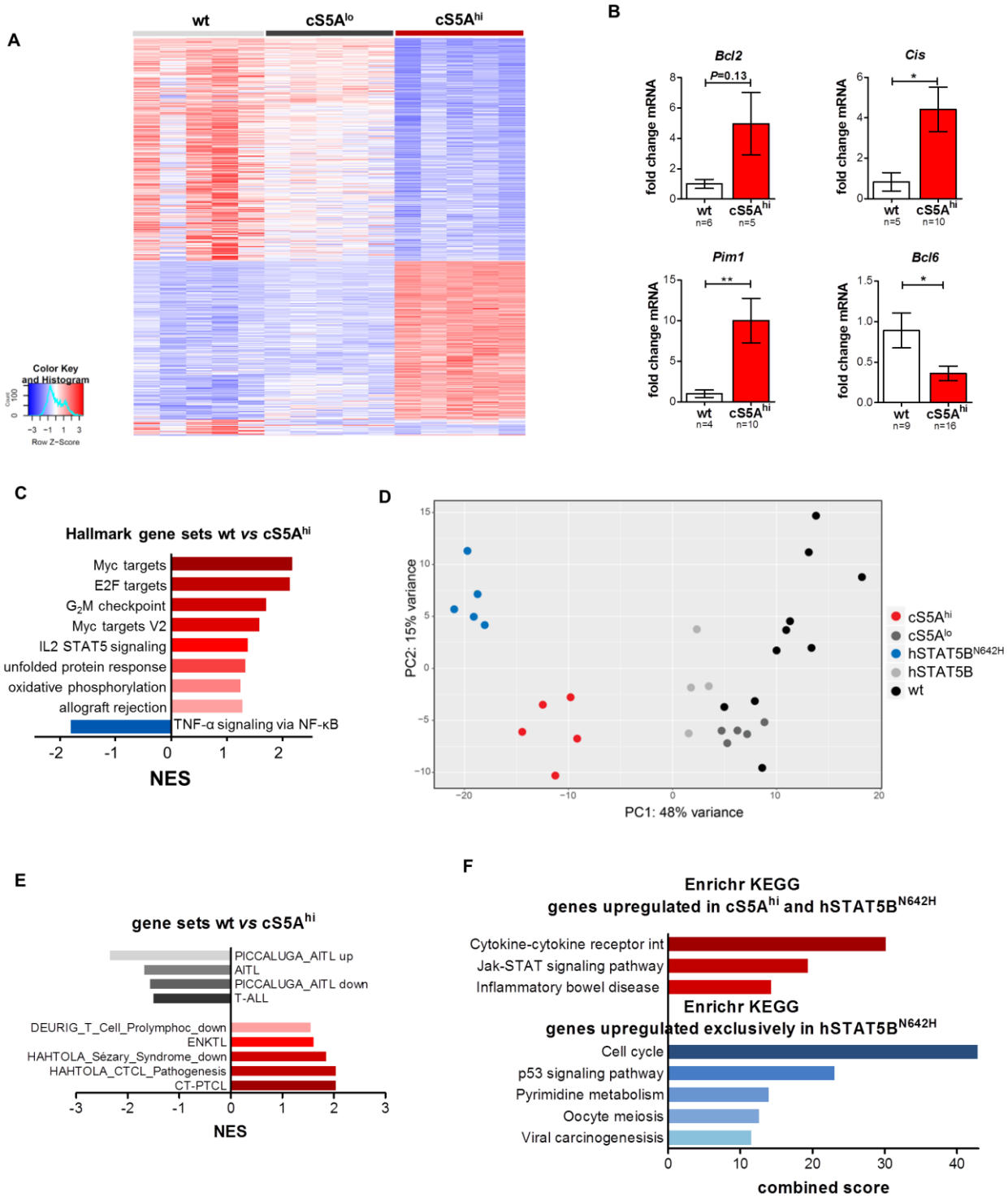

Supplementary Figure 5. Expression signature in cS5A^{F} mice

A. RNA-seq heatmap of genes deregulated in comparison of wt, cS5A^{lo} and cS5A^{hi} CD8^{+} T-cells. B. qRT-PCR validation of STAT5 T-cell target genes on mRNA isolated from lymph nodes of diseased cS5A^{hi} and age-matched wt mice (*Bcl2* P=0.13, *Cish* P=0.011, *Pim1* P=0.01, all unpaired t-test with Welch's correction, *Bcl6* P=0.015, unpaired t-test). C. Summary of gene set enrichment analysis (GSEA) of hallmark gene sets enriched in cS5A^{hi} *vs* wt CD8^{+} T-cells. D. Principal component analysis of RNA-seq data of all five genotypes analyzed, wt (n=10), hSTAT5B (n=4), hSTAT5B^{N642H}, cS5A^{lo} and cS5A^{hi} (all n=5). E. Summary of GSEA of T-cell leukemia/lymphoma gene sets positively or

negatively enriched in wt vs cS5A^{hi} CD8^{+} T-cells (false discovery rate [FDR] ≤0.25, adj. p-value ≤0.05). F. Summary of Enrichr pathways (KEGG 2016) of genes commonly upregulated in cS5A^{hi} and hSTAT5B^{N642H} or exclusively in hSTAT5B^{N642H} CD8^{+} T-cells, the list of genes can be found in Supplementary Table S5 (only adj. *P*-value≤.0.05, combined score is log(*P*-value) x Z-score).

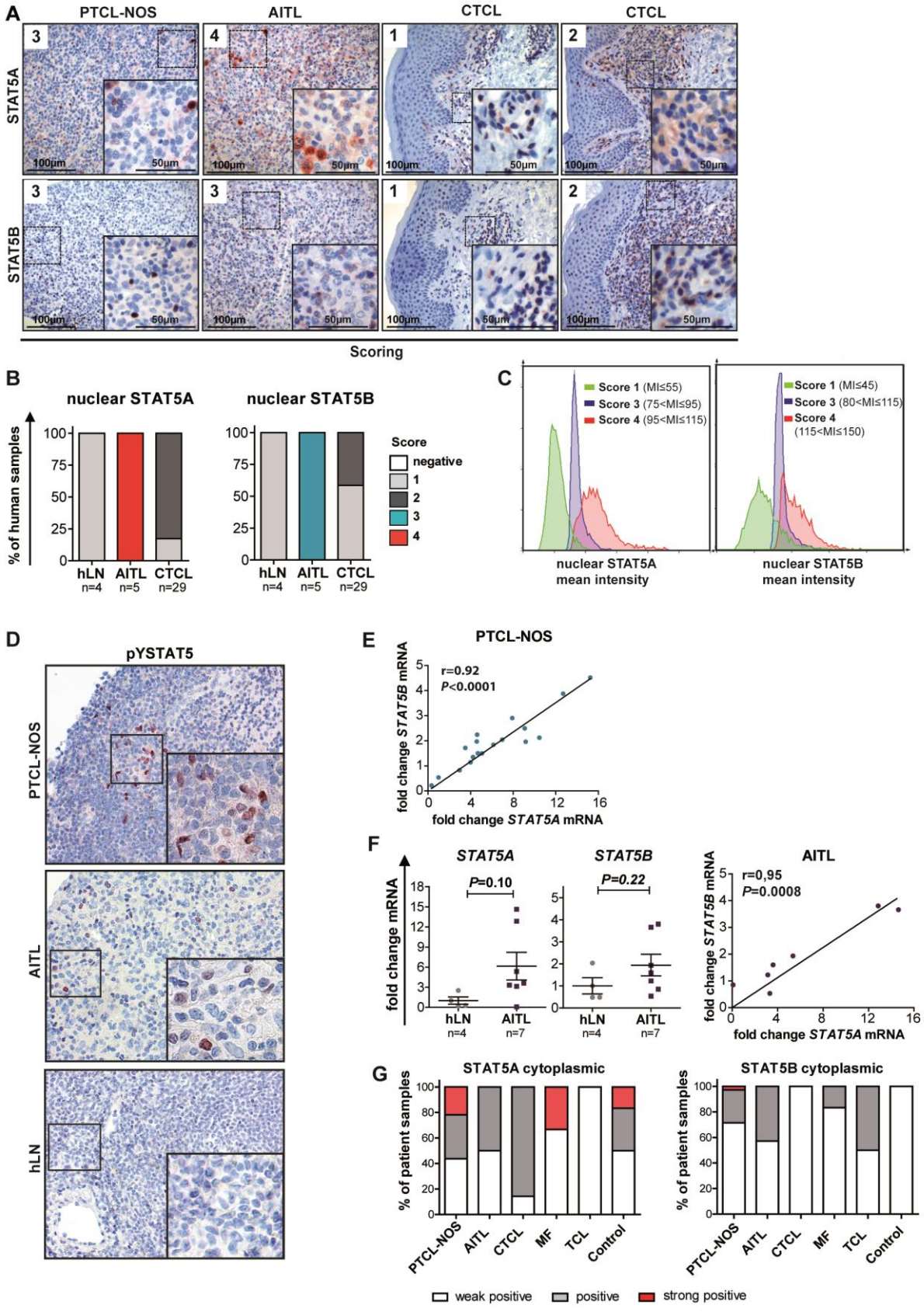

Supplementary Figure 6. Expression of STAT5 in PTCL cases

A. STAT5A (top) and STAT5B (bottom) staining of representative PTCL, NOS; AITL; and Cutaneous T-Cell Lymphoma (CTCL) cases with nuclear STAT5A/B staining intensity as summarized in B. Scale bars, 100 or 50 µm. B. Scoring summary of nuclear STAT5A (left) and

STAT5B (right) staining intensity ranging from 1 (low) to 4 (high) in AITL (*n*=5) and CTCL, (*n*=29 comprising Mycosis Fungoides (MF), Sézary Syndrome and Lymphomatoid Papulosis). C. Histograms from image analysis based quantification of nuclear STAT5A (left) and nuclear STAT5B (right) staining intensity in the representative images from Figure 8A. Mean intensity (MI) scoring zones are depicted. D. pYSTAT5 staining of PTCL, NOS and AITL case with nuclear STAT5A/B staining intensity 4 and healthy lymph node (hLN) control. E. Positive correlation (right) of *STAT5A* and *STAT5B* mRNA expression in PTCL, NOS cases (Pearson correlation r=0.92, *P*<0.0001). F. *STAT5A* (left) and *STAT5B* (middle) mRNA levels of non-diseased human lymph nodes (hLN, *n*=4) versus AITL lymphoma tissue (*n*=7, *STAT5A P*=0.10, *STAT5B P*=0.22, unpaired t-test). Mean *STAT5A* or *STAT5B* expression in hLN was normalized to 1. Positive correlation (right) of *STAT5A* and *STAT5B* mRNA expression in AITL cases (Pearson correlation r=0.95, *P*=0.0008). G. Statistical summary showing cytoplasmic STAT5A (left) and STAT5B (right) staining intensity, classified as weak positive, positive and strong positive) of 35 PTCL, NOS, 14 AITL, 7 CTCL, 6 MF, and 5 control samples spotted on a tissue microarray.

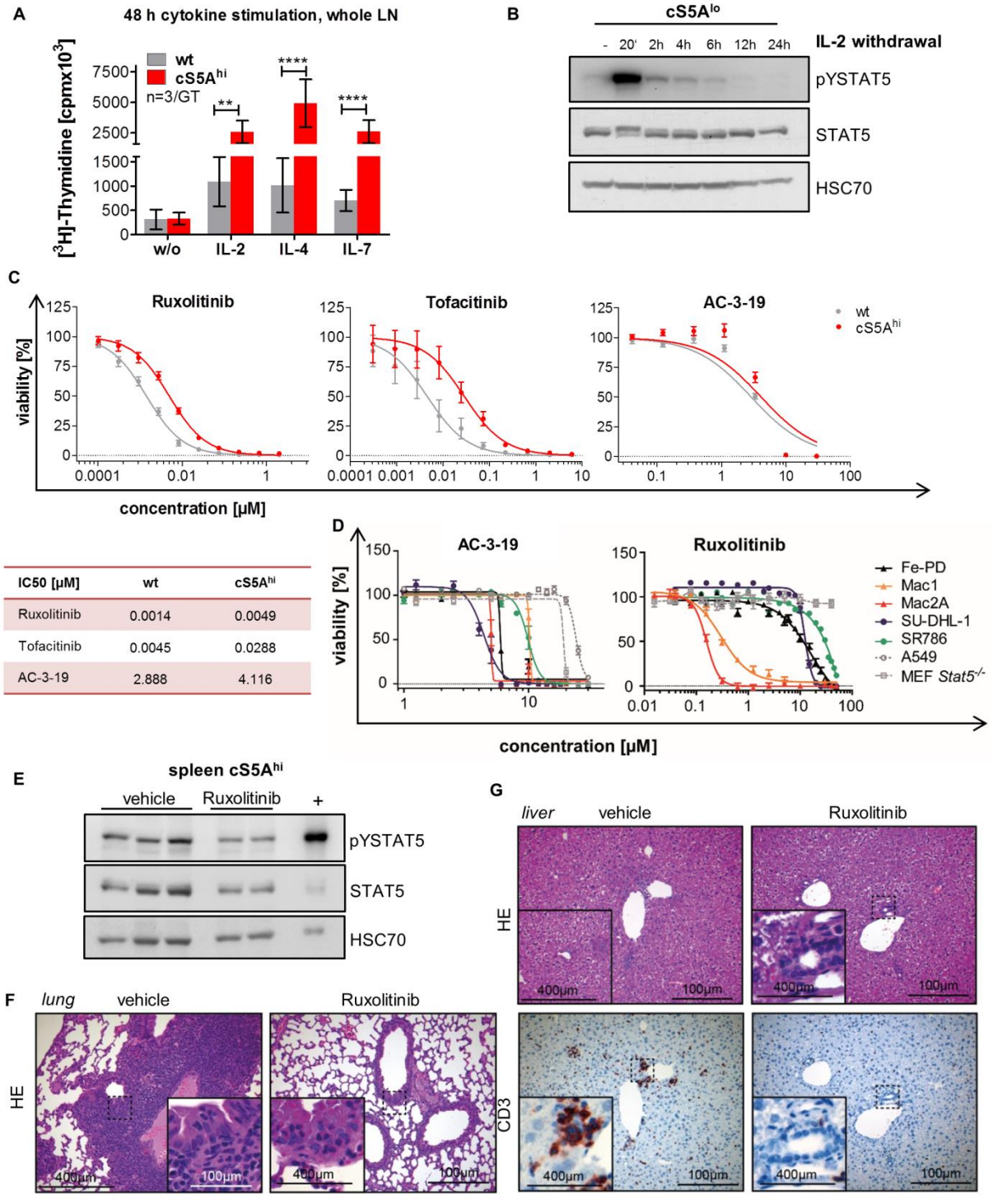

Supplementary Figure 7. Blockage of JAK/STAT signaling

A. Lymph node cells of 35-week-old wt and cS5A^{hi} mice were stimulated with IL-2 (100 U/ml, P=0.0011), IL-4 (100 ng/ml, $P \leq 0.0001$), IL-7 (10 ng/ml, $P \leq 0.0001$) or no cytokine (n.s.) for 48 h and [^{3}H]thymidine incorporation was measured (n=3/genotype in triplicates, all unpaired t-test). B. Western blot for pYSTAT5 and STAT5 on lysates of IL-2-cultured cS5A^{lo} lymph node cells sampled at specific time points after IL-2 withdrawal. HSC70 was used as loading control. C. (Top) Viability assay for cS5A^{hi} and wt CD8$^+$ T-cells (n=3/genotype) treated in triplicates with Ruxolitinib, Tofacitinib, AC-3-19, 1 µM Bortezomib (positive control set to 0 % cell viability) or DMSO (negative control) in the presence of IL-2 for 72 h. Cell viability was analyzed using CellTiter Glo Assay

(Promega). IC_{50} values (μM) were determined using GraphPad Prism 5 software (GraphPad Software, Inc.), (bottom) numerical summary of the mean IC_{50} values. D. Human PTCL cell lines (Alk^- lines Fe-PD, Mac1 and Mac2A, Alk^+ lines SU-DHL-1 and SR-786) treated with AC-3-19 (left) or Ruxolitinib (right) for 72 h ($n \geq 3$, neg. Control DMSO, 1 μM Bortezomib - positive control set to 0 % cell viability). The KRAS-transformed lung carcinoma cell line A549 cells and *Stat5*$^{-/-}$ mouse embryonic fibroblasts (MEFs) were used as control cell lines. Cell viability was measured by CellTiter Glo Assay and IC_{50} values (μM) were determined using GraphPad Prism 5 software (GraphPad Software, Inc.). E. Western blot on spleen lysates of vehicle or Ruxolitinib treated $cS5A^{hi}$ mice for pYSTAT5 and STAT5, HSC70 was used as loading control and diseased $cS5A^{hi}$ spleen lysate was used as positive control. F. HE staining on lung sections of vehicle or Ruxolitinib treated $cS5A^{hi}$ mice, scale bars represent 400 or 100 μm. G. Histological analysis (Hematoxylin and Eosin (HE) and anti-CD3 staining) on representative liver areas of vehicle or Ruxolitinib treated $cS5A^{hi}$ mice. Scale bars represent 400 or 100 μm, respectively.

Supplementary Methods

Generation of cS5A^{F} transgenic mice

We used the *vav-hCD4* hematopoietic vector *(HS21/45)*[1] and removed the *hCD4* insert with restriction endonucleases *SfiI* and *NotI*. The *hCD4* cassette was replaced by *cS5^{F}-FLAG* cDNA taken from *pMSCV-cS5^{F}-FLAG-hCD2*.[2] For this, the *cS5^{F}* cDNA was excised with *EcoRI* and subcloned into the plasmid *pBluescript II KS (-)* (restriction enzymes were purchased from eBioscience, Santa Clara, California, USA, or Fermentas, Waltham, Massachusetts, USA). This plasmid contained an *EcoRI* site followed by a *NotI* site in the multiple cloning site. cS5^{F} was ligated into *EcoRI* and the *NotI* site was located at the 3' end of the insert. The *SfiI* site was introduced by PCR. The final *vav*-cS5^{F}-construct (cS5A^{F}) was confirmed by restriction digestion (*EcoRI*, *KpnI*, *BamHI* and *HindIII*) and sequencing of the *cS5^{F}* insert. All primers used are listed in Supplementary Table S1. The cS5A^{F} construct was linearized with *HindIII* restriction digestion and gel-purified for pronuclear injection in C57BL/6N zygotes. Embryos were implanted into pseudo-pregnant females. A founder animal was identified by genotyping PCR and Southern blot analysis using DNA isolated from tail biopsies. Genomic PCR was performed with AmpliTaq® DNA Polymerase (Applied Biosystems, Foster City, California, USA) on a Mastercycler (Eppendorf, Hamburg, Germany) using transgene specific primers generating a 952 bp PCR amplification fragment in transgenics and no fragment in wt mice. For Southern blotting, genomic DNA was digested with *EcoRI* hybridizing with exon 14 of endogenous *Stat5a* as DNA probe. Transgene presence led to two fragments of 4.7 and 2.4 kb size (wt only 4.7 kb fragment). Two founder lines transmitted to the germline establishing the cS5A^{lo} [B6N-Tg(Vav-cS5F)564Biat] and cS5A^{hi} [B6N-Tg(Vav-cS5F)565Biat]cohorts. Southern blotting of offspring was used to compare signal intensities of transgene fragments. Mice were viable, fertile and kept on C57BL/6N background.

Testing cS5A^{F} *in vitro*

The IL-3 dependent murine B-cell progenitor cell line Ba/F3 was used for testing the cS5A^{F} construct *in vitro*. For electroporation, Ba/F3 cells were re-suspended in a density of 5x10^{6} cells/800 µl RPMI-1640 without supplements. Electroporation cuvettes with *HindIII* linearized cS5A^{F} plasmid DNA and cells were incubated for 5 min at room temperature, put on ice and electroporated at 300 V and 960 µF on a Gene Pulser Xcell™ (Bio-Rad, Hercules, California, USA) and grown in complete RPMI-1640 medium with or without IL-3 (2 ng/ml, ImmunoTools, Friesoythe, Germany) for transgene expression analysis.

Cell Culture

Cells were grown at 37°C and 5% CO_2 in standard medium (RPMI1640 or DMEM, details below).

Murine cell lines: Ba/F3 cells and its derivatives expressing cS5A^{F} or BCR-ABL p210[3] were cultured in RPMI-1640 medium supplemented with 10% FCS, L-Glutamine (2 mM), penicillin/streptomycin (10 U/ml) (all Gibco, ThermoFisher, Waltham, Massachusetts, USA) with or without IL-3 (2 ng/ml,

ImmunoTools, Friesoythe, Germany). E.G7-OVA and MC-38 cells were kept in RPMI-1640 medium with supplements as described for Ba/F3 cells and 0.05 mM β-Mercaptoethanol (Gibco). *Stat5*$^{-/-}$ MEFs were prepared from day E13.5-14.5 embryos from *STAT5ab*$^{+/-}$ mice[4] by mincing the carcass after removal of head and internal organs, digesting in 0.05% trypsin/0.53 mM EDTA (Gibco) for 10 min at 37 °C, re-suspending in complete growth medium (high glucose DMEM with 10% FCS, 2 mM L-Glutamine, 100 U/ml Penicillin-Streptomycin, 10 µg/ml Gentamicin, 0.1 M MEM Non-Essential Amino Acids, 55 µM β-Mercaptoethanol, all Gibco) and grown until confluent. The cS5A^{hi} CTL lines were established from lymph node single cells suspensions from diseased cS5A^{hi} mice in presence of 1 µg/ml anti-mouse CD3e (BD Pharmingen, Purified NA/LE hamster anti-mouse, Franklin Lakes, New Jersey, USA) and 100 U/ml IL-2 (ImmunoTools), corresponding wt T-cells were kept in culture for 2 weeks. Murine CTLs were grown in complete RPMI-1640 medium (10% FCS, 2 mM L-Glutamine, 10 U/ml Penicillin/Streptomycin; all Gibo) containing in addition 10 mM HEPES, 1xMEM Non-Essential Amino Acids, 50 µM β-Mercaptoethanol (all Gibco), 1 mM Sodium Pyruvate (Sigma-Aldrich, St. Louis, Missouri, USA), and 100 U/ml IL-2 (ImmunoTools). Medium was exchanged twice/week and CD8 and CD3e surface marker expression was checked regularly using flow cytometry.

Human cell lines: SR-786 (ACC-369) and SU-DHL-1 (ACC-356; both ALK^{+} ALCL) were from DSMZ (Braunschweig, Germany). Fe-PD (ALK^{-} ALCL), Mac1 and Mac2A were obtained from O.M. The lung carcinoma cell line A549 was supplied from ATCC. Mac1/2A cells have been derived from the same donor patient, Mac1 were established in the indolent cutaneous lymphoma phase, while Mac2A were established in advanced disease stage from cutaneous tumor nodules with anaplastic morphology (ALK^{-} ALCL).[5, 6] Human cell lines were grown in complete RPMI-1640 medium with 10 mM HEPES (Gibco).

mRNA isolation and qRT-PCR

For murine cells, mRNA was isolated from cell pellets using TRIzol® (Invitrogen, ThermoFisher, Waltham, Massachusetts, USA). For patient derived samples, deparaffinization of formalin-fixed, paraffin embedded (FFPE) sections was performed using xylol extraction (Sigma) followed by isolation of RNA using the miRNeasy kit (Qiagen, Hilden, Germany) according to manufacturer's protocol. First strand cDNA synthesis from isolated RNA was done using the RevertAid™ H Minus First Strand cDNA Synthesis Kit (Fermentas) using gene specific primers for FFPE samples (see supplementary Table S1). qRT-PCR was performed on a RealPexcycler (Eppendorf) using SYBR green (Roche, Basel, Switzerland) incorporation and mRNA levels were normalized for murine or human *Glyceraldehyde 3-phosphate dehydrogenase* (*Gapdh*), respectively. PTCL FFPE samples with *GAPDH* ΔCt values >30 were excluded (RNA degradation). Relative fold expression was calculated using the ΔCt method. Primer pairs are listed in Supplementary Table S1.

Immunohistochemistry

Mouse organs were fixed overnight in 4% phosphate buffered formaldehyde solution (Roti® Histofix, Carl Roth, Karlsruhe, Germany), dehydrated, paraffin embedded and cut. For immunohistochemical stainings, heat-mediated antigen retrieval was performed in citrate buffer at pH 6.0 (S1699; Dako, Agilent Technologies, Santa Clara, California, USA) and stained with antibodies against CD3, and Ki67 (listed in Supplementary Table S4) using standard protocols.

Human lymphoma cases were incubated overnight at 4 °C with STAT5A, STAT5B, or pYSTAT5 antibodies (listed in Supplementary Table S4). For STAT5A and STAT5B, a polymer-based detection system was used (Lab Vision™ UltraVision™ LP Detection System, Thermo Scientific), for pYSTAT5 an Avidin-Biotin system was used. The specific signals were amplified with AEC under visual control followed by counterstaining with Hemalaun.

For Ki67 and CD3 quantification, at least five different high-power field sections (x200 objective) of infiltrated organ areas or corresponding wildtype (wt) areas per mouse and genotype were compared using HistoQuest (TissueGnostics GmbH, Vienna, Austria) quantification software as described.[7] For nuclear STAT5A/B staining intensity quantification, high-power field sections (x200 objective) were obtained for each sample and analyzed with HistoQuest or StrataQuest (TissueGnostics GmbH) quantification software as described.[7] In brief, cut-offs (to differentiate between positive and negative cells) were set for all samples and the resulting positive nuclear STAT5A/B intensities were normalized to Hemalaun staining intensity and used for scoring based on the following intervals: STAT5A score 1 MI≤55, score 2 55<MI≤75, sore 3 75<MI≤95, score 4 95<MI≤115; STAT5B score 1 MI≤45, score 2 45<MI≤80, sore 3 80<MI≤115, score 4 115<MI≤150 or scoring weak positive, positive, strong positive.

RNA-seq processing, analysis and gene set enrichment analysis

$CD8^+$ T-cells were enriched using $CD8^+$ Magnisort kit (eBioscience, Santa Clara, California, USA) and mRNA was isolated using Trizol (Sigma-Aldrich, St. Louis, Missouri, USA) in combination with RNeasy mini kit (Qiagen, Hilden, Germany). mRNA library preparation (SENSE mRNA-Seq Library preparation) and RNA sequencing was performed with Illumina HiSeq-2500 at VBCF NGS Unit (www.vbcf.ac.at). Adapter trimming and removal of low quality bases was performed using cutadapt. After alignment of reads against contaminating sequences (mitochondrial and ribosomal DNA) remaining reads were aligned against GRCm37 using transcriptome guided alignment with TopHat version 1.4.1. Following, htseq-count with mode union was used to get gene counts for union gene models. Then differentially expressed genes (log2 fold change > 2 and FDR q-adjust < 0.1) were determined using DESeq2 version 1.12.4.

For heatmaps, centered and scaled rlog transformed library size normalized counts were visualized using the heatmap.2 function of R package gplots version 3.0.1.

For pathway analysis, the Enrichr[8] web tool was applied. The command-line version of GSEA was used for gene-set enrichment analysis (GSEA),[9, 10] and log-2 fold changes between control and experimental condition were used as ranking metric.

Gene sets were downloaded from the Molecular Signature Database v5.0 (http://www.broadinstitute.org/gsea/msigdb/index.jsp) or compiled from literature.[11, 12]

Hematocytometry and flow cytometry

Blood was obtained by tail incisions or *vena facialis* puncture collected in EDTA-tubes (Mini-Collect K3EDTA tubes, Greiner Bio-One, Kremsmuenster, Austria) and smears were stained using Modified Wright Staining. White blood cell count and hematocrit were measured using an animal blood counter (sciI Vet abc, Viernheim, Germany). For flow cytometry, erythrocytes were lysed using Gay's solution (10 mM $KHCO_3$ and 75 mM NH_4Cl, pH 7.4). Flow cytometry was used in order to determine cellular components of lymph nodes, thymus, bone marrow and spleen. Single cell suspensions were prepared by mincing organs through a 70 µm-cell strainer (BD Biosciences, Franklin Lakes, USA). All antibodies used in this study are listed in Supplementary Table S3. All analyses were performed on the BD FACS Canto II™ instrument and calculated with FACSDiva software (BD Biosciences) or FlowJo.

Viability assay

5×10^3 murine or human cells were seeded in triplicates in 96-well plates. In case of murine cells, 100 U/ml IL-2 was present in the medium. The STAT5 inhibitor AC-3-19, Ruxolitinib (Cayman Chemical Company, Ann Arbor, USA), Tofacitinib or 1 µM Bortezomib (both Selleckchem, Houston, USA) was added for 72 h. Bortezomib served as positive control for cell death (well set to 0 % viability). CellTiter-Blue® or CellTiter-Glo® (Promega, Madison, USA) reagent was used to determine viability measured on an EnSpire plate reader (PerkinElmer, Waltham, USA). IC_{50} values were determined using GraphPad Prism® 5 (GraphPad Software, San Diego, California) by non-linear regression.

Western blotting

Western blotting was done according to standard methods. Nitrocellulose membranes (Amersham™ Protran, GE Healthcare, Chicago, USA) were incubated with antibodies listed in Supplementary Table S2. HSC70 or β-ACTIN served as loading control.

MACS and FACS sorting

Magnetic cell sorting (MACS) was done on single cell suspensions prepared from lymph nodes or spleens using CD4 (L3T4), CD8a (Ly-2), CD19 or CD49b (DX5) microbeads (all anti-mouse and purchased from Miltenyi Biotec, Bergisch Gladbach, Germany) following instructions. FACS sorting of spleen and bone marrow cells or MACS-sorted, 5 days cultured NK cells was performed at 4°C on a FACSAriaII (BD Biosciences) equipped with a 488, 561, 633 and 395 nm laser and FACSDiva software (BD Biosciences) using CD4, CD8, CD19, CD11b, CD3e and NK1.1 antibodies.

Intracellular staining

Intracellular staining of FOXP3 on spleen and lymph nodes was carried out using the T_{reg} staining buffer kit (eBioscience Santa Clara, California, USA) and CD4, CD8 and CD25 antibodies (listed in Supplementary Table S3).

E.G7-OVA and MC-38 tumor growth

$1x10^6$ or $1x10^5$ E.G7-OVA or MC-38 in 100 µl PBS were injected s.c. into both flanks of 10-week-old wt, $cS5A^{lo}$ and $cS5A^{hi}$ mice, which were monitored daily. Tumor weights were determined 12 (for $1x10^6$ cells), 24 (for $1x10^5$ cells) or 18 days (MC-38) after injection.

[^{3}H]-thymidine incorporation assay

[^{3}H]-thymidine incorporation assay was done as described previously.[13] In brief, 5×10^4 lymph nodes cells or $CD8^+$ MACS sorted splenic T-cells isolated from 25-week-old wt and $cS5A^{hi}$ mice were plated in triplicates in 96 well plates in the presence of 0.1 µCi/well [^{3}H]-thymidine (PerkinElmer, Waltham, Massachusetts, USA) supplemented with IL-2 (100 U/ml, Proleukin®, Novartis, Basel, Switzerland), IL-4 (100 ng/ml, 404-ML), IL-7 (10 ng/ml, both R&D Systems, Minneapolis, USA) or without cytokines for 48 h. Incorporated radioactive counts were measured using TopCount NXT Microplate Scintillation and Luminescence Counter (PerkinElmer, Waltham, Massachusetts, USA).

$CD8^+$ T-cell transfer

$CD8^+$ T-cells were isolated by positive MACS separation (see section MACS sorting) from single cell suspensions of lymph nodes or spleens. $2x10^6$ cells were injected i.v. into $Ly5.1^+$ mice (two recipients/organ). In four-week-intervals, blood parameters were measured (scil Vet abc, Viernheim, Germany) and flow cytometric staining was performed to follow the donor-derived cell contribution. Diseased mice were euthanized, hematopoietic organs and peripheral blood analyzed using flow cytometry (CD4, CD8, CD3e, Ly5.1, Ly5.2) for the contribution of $Ly5.1^+$ and $Ly5.2^+$ cells to T-cells. Histopathology of spleen, lung, liver, kidney and pancreas was performed using HE and CD3 staining.

***In vivo* Ruxolitinib treatment**

25 weeks old $cS5A^{hi}$ mice were treated with Ruxolitinib (Chemietek, Indianapolis, Indiana) twice a day at 45 mg/kg dosage via oral gavage for 30 days. Ruxolitinib was dissolved in DMSO (Sigma-Aldrich. St, Louis, Missouri, USA) and subsequently diluted in 0.5% methylcellulose (w/v, Sigma-Aldrich).

Supplementary Tables

Supplementary Table S1: Primers

All primers were obtained from Eurofins MWG/Operon (Ebersberg, Germany). All sequences are written in 5' to 3' direction.

Primers for PCR (cloning)	
SfiIStat5a for	GCAGGCCCGTACGGCCGAATTCGACTCACAACCCCAG
BclIStat5a rev	GCAAACTGAGCTTGGATCCG
NotIER rev	GCATCAGCGCGGCCGCCCGCGGTCAGATCGTGTTG
Southern blotting primers	
Stat5a-exon 14 for	GGCAGGGTGCCATTTGCTGTG
Stat5a-exon 14 rev	CCGGTTGAACTGGGACCAGGA
Genotyping Primers	
cS5 frw	AGGCGACCATCATCAGCGAGC
cS5 rev	GAATGGAGAAATCTCGCGTCG
qPCR primers - murine	
Gapdh frw	AGAAGGTGGTGAAGCAGGCATC
Gapdh rev	CGGCATCGAAGGTGGAAGAGTG
Stat5a frw	ACGCCGGCCCATGGACAGTC
FLAG rev	CTTGTCATCGTCGTCCTTGTAGTC
Stat5a for	CGAAGCCAACAATTGCAGC
Stat5a rev	TCTCCGTGTCCTGTGTGATCAG
Bcl2 frw	ACTGAGTACCTGAACCGGCATC
Bcl2 rev	GGAGAAATCAAACAGAGGTCGC
Bcl6 frw	GATACAGCTGTCAGCCGGG
Bcl6 rev	AGTTTCTAGGAAAGGCCGGA
Cis frw	CTGGACTCTAACTGCTTGTC
Cis rev	TAGGCAGCACCGAGTCAC
Pim1 frw	TTCTCCACCGCGACATCAA
Pim1 rev	TAGCGAATCCACTCTGGAGGAC
qPCR primers - human	
STAT5a frw	TCTCCTCTGACTTCAACAGCG
STAT5a rev	ACCACCCTGTTGCTGTAGCC
STAT5a_RevTrans1	AGGGGGCGAGAGGCGGGAG
STAT5b frw	GATCAAGCAAGTGGTCCC
STAT5 rev	CCAGATCGAAGTCCCCATCGG
STAT5b_RevTrans1	CCGCGCTACGTCCATTGTG
GAPDH frw	TCTTTTGCGTCGCCAGCCGAG
GAPDH rev	GCGCCCAATACGACCAAATCCGTT
GAPDH_RevTrans1	TGACCAGGCGCCCAATACGAC

Supplementary Table S2: Western Blot Antibodies

Antibody	Company	Catalogue No.	Dilution
Monoclonal rabbit anti-mouse phospho-Stat5	Invitrogen (Calrsbad, California, USA)	716900	1:1,000
Monoclonal mouse anti-FLAG	Sigma-Aldrich (St. Louis, Missouri, USA)	F3165	1:2,000
Polyclonal rabbit anti-Stat5 (N-20)	Santa Cruz (Dallas, Texas, USA)	Sc-836	1:5,000
Monoclonal Rabbit anti-STAT5A antibody	Epitomics (Burlingame, California, USA)	1289-1	1:1,000
Polyclonal rabbit anti-mouse Stat5a	Self-made rabbit serum against the extreme C-terminus		1:5,000
Monoclonal mouse anti-mouse HSC-70	Santa Cruz(Dallas, Texas, USA)	sc-7298	1:10,000
Purified mouse anti-Stat5 antibody	Becton Dickinson (Franklin Lakes, New Jersey, USA)	610191	1:2,000
Monoclonal mouse anti-mouse β-actin	Sigma-Aldrich (St. Louis, Missouri, USA)	A5136	1:50,000
α-Tubulin	Santa Cruz (Dallas, Texas, USA)	Sc-32293	1:10,000
ECL™ Anti-mouse IgG, Horseradish Peroxidase linked whole antibody (from sheep)	GE Healthcare (Chicago, Illinois, USA)	NA931V	1:10,000
ECL™ Anti-rabbit IgG, Horseradish Peroxidase linked whole antibody (from sheep)	GE Healthcare (Chicago, Illinois, USA)	NA934V	1:10,000

Supplementary Table S3: Flow Cytometry Antibodies

All antibodies were obtained from eBioscience (Santa Clara, California, USA) unless indicated otherwise.

Antigen	Fluorochrome	Catalogue No.
CD117 (c-Kit)	PE-Cy5, APC	15-1171-83, 17-1171-82
CD11b	FITC, eFluor® 450	11-0112-82, 48-0112-82
CD16/32 (Fc-block)	Unconjugated, PE	14-0161-82, 12-0161-81
CD19	PE, eFluor® 450	12-0193-82, 48-0193-82
CD197 (CCR7)	eFluor® 450	48-1971-80
CD2	PE	12-0021-81
CD25	APC	17-0251-81
CD27	PE	12-0271-82
CD3	eFluor® 450	48-0032-82
CD3e	PerCP Cy5.5	45-0031-82
CD4	FITC, PE	11-0041-82, 12-0041-82
CD44	PE	12-0441-82
CD45.1 (Ly5.1)	PE	12-0453-82
CD45.2 (Ly5.2)	APC	17-0454-82
CD45R (B220)	eFluor® 450, PerCP Cy5.5	48-0452-82, 45-0452-82
CD49b	APC, APC-eFluor® 780	17-5971-82, 47-5971-82
CD5	APC	17-0051-81
CD62L	APC	17-0621-81
CD8a	FITC, PE, PerCP Cy5.5, APC	11-0081-82, 12-0081-82, 45-0081-82, 17-0081-82
FOXP3	PE	12-5773-80A
Lineage Panel	Biotinylated, APC-Cy7 or eFluor® 450	BD 559971
Ly6.G	APC	17-9668-80
Ly6.G (Gr1)	APC, eFluor® 450	17-5931-82, 48-5931-82
Ly-6A/E (Sca-1)	PE-Cy7, FITC	25-5981-82, 11-5981-81
NK1.1	PE-Cyanine7	25-5941-82
Streptavidin	PerCP Cy5.5, APC-eFluor® 780	45-4317-82, 47-4317-82
TER-119	eFluor 450	48-5921-82
TCRγδ	FITC	11-5711-81

Supplementary Table S4: Immunohistochemistry Antibodies

Antibody	Company	Catalogue No.	Dilution
CD3	ThermoFisher Scientific (Waltham, Massachusetts, USA)	RM-9107-S0	1:300
Ki67	Novocastra, Leica Biosystems (Wetzlar, Germany)	NCL-Ki67p	1:1,000
STAT5A	Epitomics (Burlingame, California, USA)	1289-1	1:50
STAT5B	Santa Cruz (Dallas, Texas, USA)	sc-1656	1:200
pYSTAT5	Cell Signaling Technologies (Danvers, Massachussets, USA)	9359	1:200

Supplementary Table S5: GSEA for PTCL-NOS with cytotoxic T-cell features (cS5A^{hi})

name	probe	rank in gene list	running ES	core enrichment	name	probe	rank in gene list	running ES	core enrichment
row_0	GZMB	1	0.081905	Yes	row_40	IL10	9134	0.080061	No
row_1	KLRC3	15	0.140442	Yes	row_41	IL21R	9172	0.078939	No
row_2	KLRC2	17	0.199820	Yes	row_42	LY96	9197	0.078748	No
row_3	KLRC4	18	0.259268	Yes	row_43	TNFRSF1A	9437	0.063726	No
row_4	TBX21	40	0.299721	Yes	row_44	CTSA	9622	0.052720	No
row_5	CCL5	46	0.339709	Yes	row_45	VSIG4	9866	0.037852	No
row_6	IL18RAP	47	0.379923	Yes	row_46	ILF2	10181	0.018401	No
row_7	FASLG	48	0.419827	Yes	row_47	CD84	10425	0.004230	No
row_8	CXCR3	86	0.448979	Yes	row_48	CD226	10728	-0.013688	No
row_9	EOMES	92	0.478837	Yes	row_49	IDO1	10802	-0.015485	No
row_10	SLAMF7	105	0.505789	Yes	row_50	FCGR3B	10882	-0.017593	No
row_11	IL2RB	139	0.528803	Yes	row_51	CTSK	11089	-0.028282	No
row_12	CX3CR1	192	0.546449	Yes	row_52	KLRB1	11431	-0.047828	No
row_13	IL10RB	232	0.563071	Yes	row_53	ILF3	11600	-0.054976	No
row_14	TNFSF14	295	0.575283	Yes	row_54	TGFBR1	11677	-0.055570	No
row_15	IFNGR1	325	0.588911	Yes	row_55	IL27RA	11727	-0.054171	No
row_16	PRF1	326	0.604561	Yes	row_56	CCR1	11788	-0.053439	No
row_17	GZMA	512	0.603479	Yes	row_57	SLAMF8	11803	-0.049460	No
row_18	TNFSF10	573	0.610325	Yes	row_58	CCL18	11835	-0.046610	No
row_19	CTSW	787	0.604775	No	row_59	CTSS	12078	-0.057981	No
row_20	CTSD	880	0.606929	No	row_60	CTSB	12200	-0.060584	No
row_21	CD47	1178	0.593344	No	row_61	CTSC	12401	-0.068123	No
row_22	FADD	1200	0.598992	No	row_62	IL1R2	12427	-0.063326	No
row_23	SH2D1A	1716	0.568427	No	row_63	KLRD1	12462	-0.059076	No
row_24	TGFB1	1920	0.559195	No	row_64	IL31RA	12575	-0.059959	No
row_25	GZMK	2056	0.554456	No	row_65	CCL8	12989	-0.080144	No
row_26	CD8B	2226	0.546972	No	row_66	IL1R1	13044	-0.074904	No
row_27	KLRK1	2266	0.548527	No	row_67	XCL2	13047	-0.066015	No
row_28	IFNAR1	2505	0.535746	No	row_68	XCL1	13048	-0.056986	No
row_29	IL2RG	4143	0.422963	No	row_69	CXCL10	13205	-0.057855	No
row_30	TNFRSF1B	4180	0.422223	No	row_70	CXCR4	13330	-0.055689	No
row_31	CD8A	4931	0.370750	No	row_71	CXCL9	13363	-0.046904	No
row_32	KIR3DL2	6549	0.257546	No	row_72	IL1RN	13650	-0.053331	No
row_33	KIR3DL3	6550	0.257546	No	row_73	TNFRSF12A	13692	-0.042076	No
row_34	KIR2DL1	6551	0.257546	No	row_74	CD244	13704	-0.028570	No
row_35	KIR2DL3	6552	0.257546	No	row_75	SLAMF6	13833	-0.021426	No
row_36	KIR3DL1	6553	0.257546	No	row_76	IL18	13950	-0.011375	No
row_37	KIR2DL4	6554	0.257546	No	row_77	IL13RA1	14005	0.004201	No
row_38	CXCL11	7701	0.177693	No	row_78	IFNGR2	14055	0.021493	No
row_39	CCL2	8835	0.099500	No					

Supplementary Table S6: Enrichr

Term	Overlap	P-value	Adj. P-value	Z-score	Combined Score	Genes
upregulated exclusively in hSTAT5B^{N642H}						
Cell cycle_Homo sapiens_hsa04110	17 of 124	1,817E-11	2,653E-09	-1,73320	42,864	SMAD3, CDKN2C, CDKN2A, PLK1, BUB1B, CDC25C, GADD45G, CDC20, CCNA2, CCNB2, CCNB1, TFDP1, CDC45, ESPL1, CHEK1, CDK1, E2F2
p53 signaling pathway_Homo sapiens_hsa04115	9 of 69	1,703E-06	0,00012	-1,73739	23,078	CCNB2, CCNB1, RRM2, CDKN2A, ZMAT3, CHEK1, CDK1, BAX, GADD45G
Pyrimidine metabolism_Homo sapiens_hsa00240	8 of 105	0,00032	0,01544	-1,73479	13,975	NT5E, UCK2, RRM2, NUDT2, TK1, TYMS, DCTPP1, NME1
Oocyte meiosis_Homo sapiens_hsa04114	8 of 123	0,00091	0,03327	-1,80427	12,631	CDC20, CCNB2, CCNB1, SGOL1, ESPL1, PLK1, CDK1, CDC25C
Viral carcinogenesis_Homo sapiens_hsa05203	10 of 205	0,00199	0,04845	-1,85515	11,537	CDC20, CCNA2, CDKN2A, CHEK1, CDK1, BAX, HIST1H2BE, HIST1H4D, CCR4, CCR3
upregulated in cS5A^{hi} and hSTAT5B^{N642H}						
Cytokine-cytokine receptor interaction_Homo sapiens_hsa04060	15 of 265	1,045E-07	1,411E-05	-1,87718	30,174	CX3CR1, CSF2, IL10RA, IL18RAP, IFNG, CXCR3, IL2RA, CCL5, IL2RB, TNFSF8, CCR5, IL18R1, CCR2, IL12RB2, BMPR1A
Jak-STAT signaling pathway_Homo sapiens_hsa04630	9 of 158	3,767E-05	0,00254	-1,90533	19,409	CSF2, CISH, IFNG, IL10RA, IL2RA, IL2RB, PIM1, BCL2, IL12RB2
Inflammatory bowel disease (IBD)_Homo sapiens_hsa05321	5 of 65	0,00054	0,02432	-1,89732	14,274	IL18RAP, IFNG, TBX21, IL18R1, IL12RB2

Supplementary Table S7: Reported mutations in human T-cell lymphoma cell lines

Cell Line	Type	JAK/STAT mutations	Other relevant mutations
SR786	ALCL cell line of T-cell type derived from pediatric $CD30^+$ lymphoma		NPM1-ALK, missense TP53
Mac1	ALCL, Mac2A sister cell line, at indolent stage - different immunological, functional features	PCM1-JAK2, JAK3 V722I	
Mac2A	ALCL cell line (of T-cell type) derived from aggressive ALCL post-Hodgkin lymphoma and post-CTCL, representing advanced skin $CD30^+$ Mycosis Fungoides	PCM1-JAK2, JAK3 V722I, SOCS1 G78R/D105N	
Su-DHL-1	ALCL cell line derived from child with malignant histiocytosis		NPM1-ALK, missense TP53 and DNMT3A mutation
Fe-PD	ALCL cell line	STAT3 G618R, JAK1 G1097V	

References

1. Ogilvy S, Metcalf D, Gibson L, Bath ML, Harris AW, Adams JM. Promoter Elements of vav Drive Transgene Expression In Vivo Throughout the Hematopoietic Compartment. Blood. 1999;94(6):1855-1863.

2. Gilbert S, Nivarthi H, Mayhew Christopher N, et al. Activated STAT5 Confers Resistance to Intestinal Injury by Increasing Intestinal Stem Cell Proliferation and Regeneration. Stem Cell Reports. 2015;4(2):209-225.

3. Friedbichler K, Kerenyi MA, Kovacic B, et al. Stat5a serine 725 and 779 phosphorylation is a prerequisite for hematopoietic transformation. Blood. 2010;116(9):1548-1558.

4. Cui Y, Riedlinger G, Miyoshi K, et al. Inactivation of Stat5 in Mouse Mammary Epithelium during Pregnancy Reveals Distinct Functions in Cell Proliferation, Survival, and Differentiation. Mol Cell Biol. 2004;24(18):8037-8047.

5. Ehrentraut S, Nagel S, Scherr ME, et al. t(8;9)(p22;p24)/PCM1-JAK2 Activates SOCS2 and SOCS3 via STAT5. PLoS One. 2013;8(1):e53767.

6. Davis TH, Morton CC, Miller-Cassman R, Balk SP, Kadin ME. Hodgkin's Disease, Lymphomatoid Papulosis, and Cutaneous T-Cell Lymphoma Derived from a Common T-Cell Clone. N Engl J Med. 1992;326(17):1115-1122.

7. Schlederer M, Mueller KM, Haybaeck J, et al. Reliable Quantification of Protein Expression and Cellular Localization in Histological Sections. PLoS One. 2014;9(7):e100822.

8. Kuleshov MV, Jones MR, Rouillard AD, et al. Enrichr: a comprehensive gene set enrichment analysis web server 2016 update. Nucleic Acids Res. 2016;44(W1):W90-W97.

9. Subramanian A, Tamayo P, Mootha V, et al. Gene set enrichment analysis: a knowledge-based approach for interpreting genome-wide expression profiles. Proc Natl Acad Sci USA. 2005;102(43):15545-15550.

10. Mootha V, Lindgren C, Eriksson K, et al. PGC-1alpha-responsive genes involved in oxidative phosphorylation are coordinately downregulated in human diabetes. Nat Genet. 2003;34(3):267-273.

11. Iqbal J, Weisenburger DD, Greiner TC, et al. Molecular signatures to improve diagnosis in peripheral T-cell lymphoma and prognostication in angioimmunoblastic T-cell lymphoma. Blood. 2010;115(5):1026-1036.

12. Iqbal J, Wright G, Wang C, et al. Gene expression signatures delineate biological and prognostic subgroups in peripheral T-cell lymphoma. Blood. 2014;123(19):2915-2923.

13. Nivarthi H, Prchal-Murphy M, Swoboda A, et al. Stat5 gene dosage in T cells modulates CD8+ T-cell homeostasis and attenuates contact hypersensitivity response in mice. Allergy. 2015;70(1):67-79.